RESEARCH ARTICLE

Highly sensitive HPLC analysis and biophysical characterization of N-glycans of IgG-Fc domain in comparison between CHO and 293 cells using FcγRIIIa ligand

Hirofumi Kosuge[1] | Satoru Nagatoishi[2] (iD) | Masato Kiyoshi[3] (iD) |
Akiko Ishii-Watabe[3] | Toru Tanaka[4] | Yosuke Terao[4] | Seigo Oe[4] |
Teruhiko Ide[4] | Kouhei Tsumoto[1,2] (iD)

[1]School of Engineering, The University of Tokyo, Tokyo, Japan

[2]The Institute of Medical Science, The University of Tokyo, Tokyo, Japan

[3]Division of Biological Chemistry and Biologicals, National Institute of Health Sciences, Kanagawa, Japan

[4]Tosoh Corporation, Kanagawa, Japan

Correspondence
Kouhei Tsumoto, School of Engineering, The University of Tokyo, 7-3-1, Hongo, Bunkyo-ku, Tokyo 113-8656, Japan.
Email: tsumoto@bioeng.t.u-tokyo.ac.jp

Funding information
Japan Society for the Promotion of Science, Grant/Award Numbers: 16H02420, 18H02082

Peer Review
The peer review history for this article is available at https://publons.com/publon/10.1002/btpr.3016.

Abstract

Quality control of monoclonal antibodies is challenging due in part to the diversity of post-translational modifications present. The regulation of the N-glycans of IgG-Fc domain is one of the key factors to maintain the safety and efficacy of antibody drugs. The FcγRIIIa affinity column is an attractive tool for the precise analysis of the N-glycans in IgG-Fc domain. We used the mutant FcγRIIIa, which is produced in *Escherichia coli* and is therefore not glycosylated, as an affinity reagent to analyze the N-glycans of monoclonal antibodies expressed in Expi293 and ExpiCHO cells. The monoclonal antibodies expressed in these cells showed very different chromatograms, because of differences in terminal galactose residues on the IgG-Fc domains. We also carried out kinetic and thermodynamic analyses to understand the interaction between monoclonal antibodies and the mutant FcγRIIIa. Expi293 cell-derived monoclonal antibodies had higher affinity for the mutant FcγRIIIa than those derived from ExpiCHO cells, due to slower off rates and lower binding entropy loss. Collectively, our results suggest that the FcγRIIIa column can be used to analyze the glycosylation of antibodies rapidly and specifically.

KEYWORDS

antibody drug, FcγRIIIa column, galactosylation, monoclonal antibody, N-glycosylation

1 | INTRODUCTION

Numerous protein drugs are now developed and marketed for treatment of various diseases.[1] Although protein drugs often have high efficacy, it is currently difficult to produce protein drugs by chemical synthesis; they are mainly produced in bacterial, yeast, insect, or mammalian cells. The quality control of protein drugs is challenging in large part due to the diversity of possible post-translational modifications.

Antibodies have high specificity and efficacy.[1-3] More than 80 antibody drugs are currently approved by FDA,[4] most to treat cancer or autoimmune diseases. Quality control of monoclonal antibodies (mAbs) is an important work to supply secure and reliable antibody drugs to patients. Measures of the quality of monoclonal antibodies include thermal stability, aggregation, degradation, and immunogenicity.[5-8] Post-translational modifications also regulate antibody activity. In particular, the N-linked glycans of the IgG-Fc domain in the constant region influence effector function of antibodies such as

antibody-dependent cellular cytotoxicity (ADCC) and complement-dependent cytotoxicity (CDC).[9-11] N-glycans affect ADCC activity because this modification of the IgG-Fc domain is an important role in the interaction between IgG and FcγRIIIa, an antibody receptor found on the surface of certain immune cells. The absence of core fucose of the N-glycans enhances the affinity of an antibody for FcγRIIIa and greatly boosts ADCC activity.[9-14] Three approved antibody drugs, mogamulizumab, obinutuzumab, and benralizumab, have a high affinity for FcγRIIIa due to the absence of fucose, resulting in high efficacy. Also, the presence of terminal galactose residues in the IgG-Fc domain frequently enhances the affinity for FcγRIIIa,[9,14-17] and N-glycans of the IgG-Fc domain affect stability, conformation, and aggregation of antibodies, as well as the effector function.[10,11,18,19]

Effector function is critical for many antibody drugs used in the treatment of cancer, including rituximab and trastuzumab.[20] On the other hand, for antibody drugs for the treatment of autoimmune diseases, effector function is not desired in general. It is a difficult issue to produce or separate antibody drugs with uniform carbohydrate modifications because the glycoforms of the IgG-Fc domain depend on cells used in production, medium components, and temperature.[21-25] For example, we showed that the N-glycan composition of trastuzumab was different when the antibody was produced in CHO cells and insect cells.[21]

Strict regulation of the glycosylation is necessary to improve and control the quality of antibody drugs. The FcγRIIIa affinity column is an attractive tool for the precise analysis of the N-glycans in IgG-Fc domain. The FcγRIIIa used as an affinity ligand is a mutant produced in *Escherichia coli* that is not glycosylated. Highly purified, medical-grade rituximab separates into three peaks when running over an FcγRIIIa column, and these peaks were attributed to the different glycan compositions.[15] Here, to evaluate the utility of the FcγRIIIa column, we used it to analyze the diversity of N-glycans of IgG1 expressed in two different cell lines.

2 | MATERIALS AND METHODS

2.1 | Expression and purification of mAbs from Expi293 and ExpiCHO cells

The DNA sequences of the heavy and light chain of rituximab and trastuzumab were subcloned into the pcDNA3.4 vector (Thermo Fisher Scientific). The vectors were transiently transfected into Expi293 cells (Thermo Fisher Scientific) using ExpiFectamine 293 Transfection Kit (Thermo Fisher Scientific) in accordance with the manufacturer's protocol. The cells were cultured for 3 to 4 days at 37°C and 8% CO_2. The cultures were centrifuged at 400g for 15 min, and the supernatant was collected.

The same vectors were transiently transfected into ExpiCHO cells (Thermo Fisher Scientific) using ExpiFectamine CHO Transfection Kit (Thermo Fisher Scientific) in accordance with the manufacturer's standard protocol. The cells were cultured for 8 days at 37°C and 8% CO_2. The cultures were centrifuged at 400g for 15 min, and the supernatant was collected.

Each supernatant was applied onto an rProtein A Sepharose Fast Flow column (GE Healthcare) equilibrated with PBS at pH 7.4. The fraction bound to the column was washed with the PBS and subsequently eluted with Pierce IgG Elution Buffer (Thermo Fisher Scientific). The eluted fraction was neutralized by addition of 2 M Tris–HCl (pH 8.0) and further purified by size exclusion chromatography using a HiLoad 16/600 Superdex 200 pg column (GE Healthcare) equilibrated with PBS at pH 7.4.

2.2 | Expression and purification of Mut FcγRIIIa

Mut FcγRIIIa has nine mutated amino acids as described previously.[15] The Mut FcγRIIIa in vector pTrc99a (GE Healthcare) has a hexahistidine tag at the C-terminus. *E. coli* strain BL21 (DE3) was transformed with the Mut FcγRIIIa expression vector and was grown overnight at 37°C in 3 ml of Luria-Bertani medium. The cells were diluted into 1 L of $2 \times YT$ medium and cultured at 37°C and until the OD_{600} reached a value of 0.5–0.6. At that point, 0.2 mM of isopropyl β-D-1-thiogalactopyranoside was added, and the cells were cultured overnight at 20°C. The cells were harvested by centrifugation at 8,000g for 10 min at 4°C. The cell pellet was resuspended in binding buffer (20 mM Tris–HCl, 500 mM NaCl, 5 mM imidazole at pH 8.0), and the cells were lysed with an ultrasonic cell-disrupting UD-201 instrument (TOMY). The cell lysate was centrifuged at 40,000g for 30 min at 4°C. The soluble fraction was collected and applied onto a Ni-NTA agarose affinity column (Qiagen) equilibrated with the binding buffer. The fraction bound to the column was first washed with binding buffer, and subsequently fractions eluted with the same buffer containing 100 and 500 mM imidazole were collected. The eluted fractions containing Mut FcγRIIIa were further purified by size exclusion chromatography using a HiLoad 16/600 Superdex 75 pg column (GE Healthcare) equilibrated with 50 mM Tris–HCl, 500 mM NaCl, 1 mM EDTA at pH 8.0.

2.3 | HPLC analysis using FcγRIIIa column

An affinity column (4.6 mm I.D. × 75 mm) packed with Mut FcγRIIIa-immobilized resin from TOSOH (Tokyo, Japan) described previously[15] were used in HPLC analyses of mAbs. HPLC analyses were conducted using an AZURA Analytical HPLC instrument (KNAUER). Mobile phase A was 20 mM sodium acetate, 50 mM NaCl at pH 5.0, and mobile phase B was 10 mM glycine-HCl at pH 3.0. For analysis, 10 μl of each sample of Expi293-Rituximab, ExpiCHO-Rituximab, Expi293-Trastuzumab, or ExpiCHO-Trastuzumab concentrated to 14 μM was loaded onto the FcγRIIIa column equilibrated with mobile phase A. A linear gradient (0 to 100% B) for 28 min and 100% mobile phase B for 10 min at a flow rate of 0.6 ml/min was used to elute the antibodies. The total run time to measure one sample including the re-equilibration process after elution is 60 min.

2.4 | Glycan analysis

The analytical method to determine the composition of the N-glycan comprised three steps: Release of N-linked oligosaccharides, labeling

with 2-aminobenzamide (2-AB), and UPLC. The N-linked oligosaccha-rides were released enzymatically using PNGase F (Roche). 20 μg of antibodies were mixed with 1 U of PNGase F. The mixture was incu-bated at 37°C for 16 hr, and the resulting digested compounds were loaded onto an Envi-Carb graphitized carbon column (Spelco) pre-treated with 1.0 ml acetonitrile. After a washing step with 3.0 ml water, the N-glycan was eluted with 1.0 ml of 5 mM ammonium ace-tate in 50% acetonitrile. The eluted fractions were collected and dried with a centrifugal evaporator (Speedvac, Thermofisher). The labeling solution (10 μl of 0.37 M 2-AB and 1 M NaCNBH$_3$ in 70:30 [v:v] DMSO:acetic acid) was added to dried samples of N-glycan. The reac-tion mixtures were incubated at 65°C for 3 hr. Acetonitrile (1 ml) was gently added to the labeled glycan sample solution, followed by cen-trifugation at 15,000g for 10 min. The supernatant was discarded, and the pellet containing the labeled glycan was dissolved in 20 μl of dis-tilled water. A total of 1 μl of glycan solution was subjected to a Waters ACQUITY UPLC BEH amide column (2.1 × 150 mm, 1.7 μm) in a Waters ACQUITY UPLC H-class system. Mobile phase A was 0.1 M ammonium formate at pH 4.6, and mobile phase B was 100% (v/v) acetonitrile. A linear gradient (A; 25% B; 75% to A; 50% B; 50%) for 50 min was applied and fluorescence signals were detected at 420 nm (Excited at 330 nm).

2.5 | Surface plasmon resonance

The interaction between each mAb and Mut FcγRIIIa was analyzed using SPR in a Biacore T200 instrument (GE Healthcare). A CM5 Biacore sen-sor chip (GE Healthcare) was activated by treatment with N-hydroxysuccinimide/N-ethyl-N′-(3-dimethylaminopropyl) carbodiimide hydrochloride, followed by immobilization of Penta·His Antibody, BSA-free (Qiagen) at 10,000–13,000 RU. After the immobilization, the acti-vated surface of the sensor chip was blocked with 1 M ethanolamine hydrochloride at pH 8.5. 10 nM Mut FcγRIIIa was injected and captured by the Penta·His Antibody for 18 s at a flow rate of 10 μl/min targeting for about 20–70 RU of capture level. The interaction between each mAb and Mut FcγRIIIa was measured by injecting each mAb into the sensor chip at a flow rate of 30 μl/min; a range of concentrations were tested. The association time was 90 s, and the dissociation time was 180 s. The assay was carried out in PBS (pH 7.4) containing 0.005% (v/v) Tween-20 at 10, 15, 20, 25, and 30°C. The capture of Mut FcγRIIIa was carried out at the beginning of each cycle, and the regeneration procedure was car-ried out with 1 M Arg-HCl at pH 4.4 at the end of each cycle. Data analy-sis was performed with the BIAevaluation software (GE Healthcare). Association rate constants (k_{on}) and dissociation rate constants (k_{off}) were determined by a global fitting analysis assuming a 1:1 Langmuir binding model. The dissociation constant (K_D) was calculated as follows:

$$K_D = k_{off}/k_{on}$$

The changes in enthalpy ($\Delta H°$) and entropy ($\Delta S°$) were calculated from the slope and intercept of the temperature dependence of the dissociation constant determined using the van't Hoff formula:

$$\ln K_D = \Delta H°/RT - \Delta S°/R$$

where R is the gas constant and T is the absolute temperature.

2.6 | Differential scanning calorimetry

Differential scanning calorimetry (DSC) measurements of each mAb were performed using an automated VP-DSC microcalorimeter (MicroCal VP-Capillary DSC, Malvern). Sample concentrations were adjusted to 10 μM in PBS (pH 7.4). Each sample was heated from 10 to 100°C at a rate of 60°C/hr. Analysis of the collected data was carried out using a non-two-state model with ORIGIN 7 software.

2.7 | Differential scanning fluorimetry

Differential scanning fluorimetry (DSF) measurements of each mAb were performed using a Real-Time PCR instrument (CFX Connect Real-Time PCR Detection System, Bio-Rad). Samples were prepared at 1 μM concentration in PBS (pH 7.4) and mixed with one-twentieth volume of SYPRO Orange (Invitrogen) that had been 50-fold diluted in water (v/v). Samples were heated from 20 to 100°C in 0.2°C incre-ments with an equilibration time of 5 s at each temperature. The melt-ing temperatures were determined using CFX Manager software (Bio-Rad).

2.8 | Circular dichroism

The secondary structure of each mAb was analyzed by the measure-ment of the circular dichroism (CD) spectrum using a J-820 spectro-polarimeter (Jasco). Samples were prepared at 0.7 μM in PBS (pH 7.4) in a 1 mm path-length quartz cell. The CD measurements were carried out at 25°C by continuous scanning from 200 to 260 nm at a scanning speed of 20 nm/min. Five scans of each sample were accumulated. Analysis of the collected data was carried out using Spectra Analysis software (Jasco).

3 | RESULTS AND DISCUSSION

3.1 | HPLC analysis of IgG1 derived from Expi293 and ExpiCHO cells using the FcγRIIIa column

We analyzed glycosylation patterns of rituximab and trastuzumab iso-lated from Expi293 and ExpiCHO cells using an FcγRIIIa affinity col-umn. The FcγRIIIa has nine mutations relative to the wild-type protein and is not glycosylated as it is produced in *E. coli*. The mAbs were loaded onto the column and eluted using a linear pH gradient. The elu-tion profiles of the four mAbs are shown in Figure 1. Each HPLC chro-matogram consisted of several peaks. In Expi293-Rituximab and Expi293-Trastuzumab chromatograms, three large peaks were
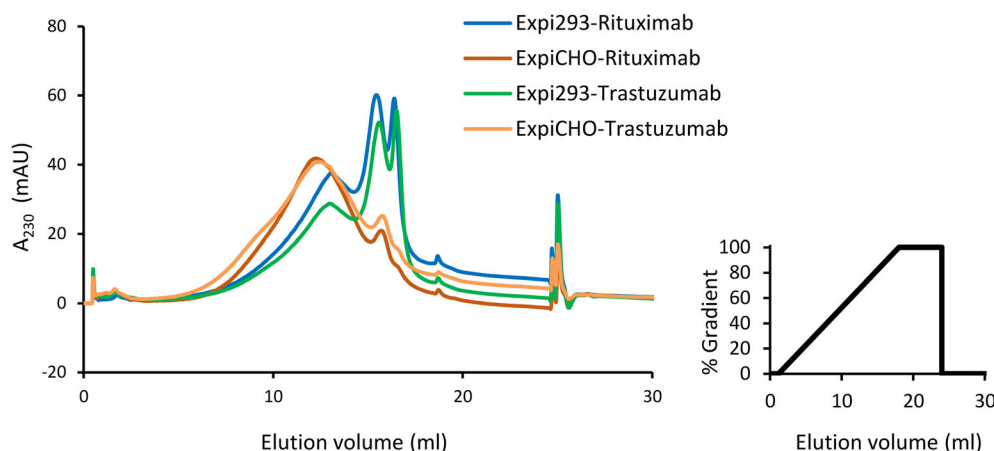
FIGURE 1 HPLC analysis of mAbs using FcγRIIIa column. HPLC chromatograms of Expi293-Rituximab (blue), ExpiCHO-Rituximab (red), Expi293-Trastuzumab (green), and ExpiCHO-Trastuzumab (yellow) monitored at 230 nm. The gradient used for the HPLC analysis is shown on the right

Glycoform	G0-N	G0F-N	G0	G0F	M5	G1F (α1, 6)	G1F (α1, 3)	G2F
Structure scheme								
Expi293-Rituximab	0	2	0	51	3	27	11	6
ExpiCHO-Rituximab	0	3	0	89	3	3	1	0
Expi293-Trastuzumab	0	2	0	51	3	26	12	6
ExpiCHO-Trastuzumab	0	3	0	85	6	4	2	0

FIGURE 2 Percentage distributions of the major glycoforms on mAbs expressed in Expi293 and ExpiCHO cells. Blue squares, green circles, yellow circles, and red triangles correspond to N-acetylglucosamine, mannose, galactose, and fucose, respectively

observed at 13.0, 15.4–15.6, and 16.4–16.5 ml elution volumes, whereas chromatograms of ExpiCHO-Rituximab and ExpiCHO-Trastuzumab each had major one peak at 12.3–12.5 ml and two small peaks at 15.7–15.8 and 16.5–16.7 ml. Thus, in general, the retention times of Expi293-Rituximab and Expi293-Trastuzumab were longer than those of ExpiCHO-Rituximab and ExpiCHO-Trastuzumab. Based on our previous report,[15] these peaks are due to populations with different glycosylation patterns, and the differences in profiles between Expi293 and ExpiCHO cell-derived mAbs suggest that the glycosylation patterns are dependent on the cell line in which the mAb was expressed. The reproducibility of the FcγRIIIa column was also succeeded in using the same lot of sample and running buffer (Figure S1).

3.2 | Glycan analysis

The glycosylation patterns of each mAb were determined. We observed different glycosylation patterns between Expi293 and ExpiCHO cell-derived mAbs, whereas there were almost no differences in glycoforms present on the mAbs derived from the same cells (Figure 2). This result explains the similarities in HPLC profiles of mAbs derived from the same cells (Figure 1). The most significant

difference between Expi293 and ExpiCHO cell-derived mAbs is in the proportions of galactose residues. Expi293 cell-derived mAbs had more N-glycans with terminal galactose residues (G2F, G1F(α1, 6), G1F(α1, 3)) than ExpiCHO cell-derived mAbs. In agreement with this finding, it was reported that antibodies expressed in HEK293 cells had N-glycans with more galactose residues than those expressed in CHO cells.[23] Although the values of $T_m 1$ (generally corresponds to the denature of CH2 domain[26]) were slightly different among trastuzumab and rituximab because of the difficulty to obtain exact values of $T_m 1$ caused by the overlap of adjacent melting peaks in DSC measurements, we did not observe significant differences of thermal stabilities (as measured by DSC and DSF) or in secondary structures (as monitored by CD) in mAbs produced in different cell lines (Figure S2, Tables S1 and S2).

3.3 | Kinetic analysis of the interaction between mAbs and Mut FcγRIIIa using SPR

To understand the interaction between mAbs and Mut FcγRIIIa used in the affinity column analysis, SPR analysis was carried out (Figure 3a). Based on curve fitting, kinetic parameters were determined (Table 1). The curve fitting profiles and Chi-squared values are shown in Figure S3. Expi293-Rituximab had higher affinity for Mut FcγRIIIa than did ExpiCHO-Rituximab, due to a slower dissociation rate. Trastuzumab derived from Expi293 cells also had higher affinity than the mAb derived from ExpiCHO cells. Our data suggest that the higher affinity of Expi293 cell-derived mAbs is due to the higher proportion of galactose residues of their N-glycans. These results of SPR analysis reflect the difference in the retention times of mAbs derived from Expi293 and ExpiCHO cells in the affinity column analysis. When rituximab and trastuzumab expressed by the same cells were compared, rituximab had a higher affinity for Mut FcγRIIIa. There are no differences in amino acid sequences in the Fc and hinge regions of these two mAbs we used (Figure S4). This result indicates that the Fab domain, as well as the IgG-Fc domain, of mAbs influences the interaction with FcγRIIIa.

FIGURE 3 Analyses of the interactions between Mut FcγRIIIa and mAbs. (a) Binding assay between Mut FcγRIIIa and mAbs expressed in Expi293 and ExpiCHO cells by SPR at 25°C. Line darkness indicates concentration with the darkest line the highest concentration. (b) Van't Hoff plots of the interaction between Mut FcγRIIIa and rituximab. At least three independent SPR measurements at each temperature were carried out. The average values of K_D at each temperature are shown. R-squared values are greater than 0.99 for both Expi293-Rituximab and ExpiCHO-Rituximab. (c) Thermodynamic parameters of the interactions between Mut FcγRIIIa and rituximab expressed in Expi293 and ExpiCHO cells. Each parameter was determined from van't Hoff plots. Standard errors of linear fitting of van't Hoff plots are shown as error bars
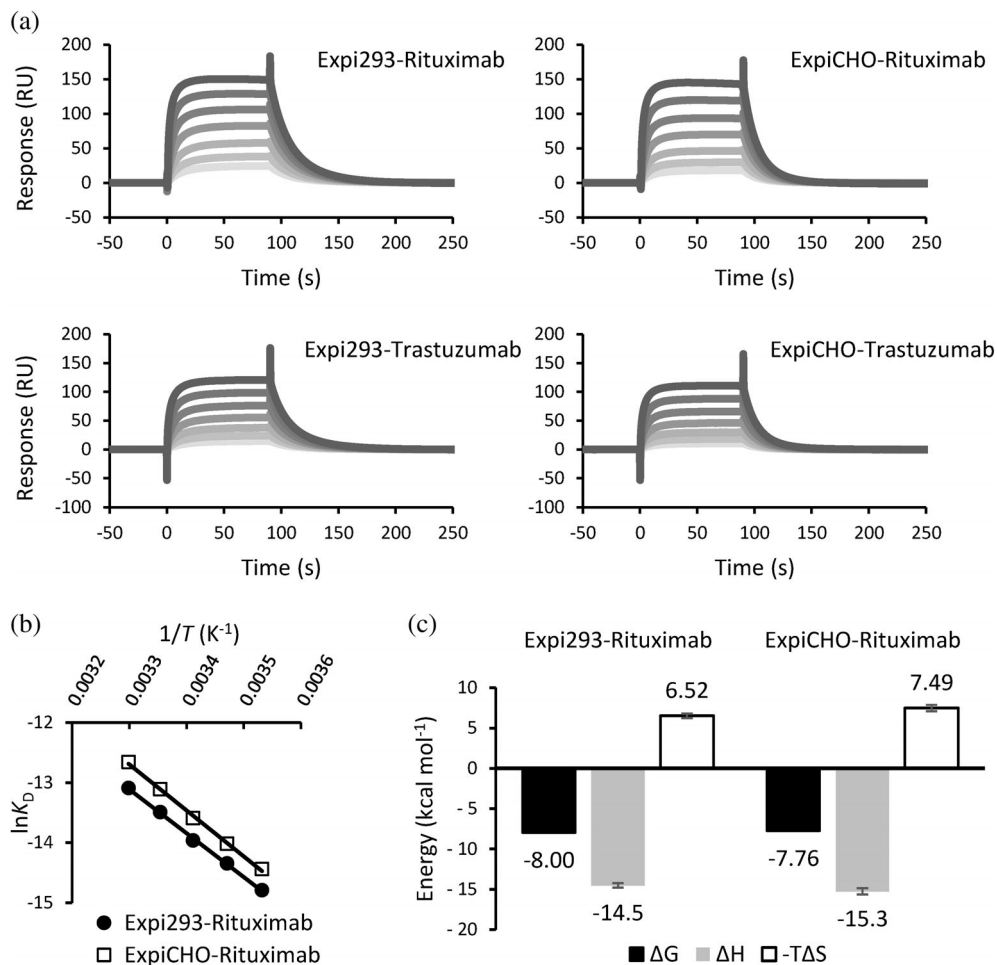

TABLE 1 Kinetic parameters of the interaction between Mut FcγRIIIa and mAb at 25°C

	k_{on} ($\times 10^4$ M^{-1} s^{-1})	k_{off} ($\times 10^{-2}$ s^{-1})	K_D ($\times 10^{-6}$ M)
Expi293-Rituximab	3.96 ± 0.11	5.44 ± 0.11	1.38 ± 0.04
ExpiCHO-Rituximab	3.99 ± 0.20	8.03 ± 0.14	2.03 ± 0.07
Expi293-Trastuzumab	3.00 ± 0.10	5.83 ± 0.16	1.95 ± 0.05
ExpiCHO-Trastuzumab	3.62 ± 0.31	8.93 ± 0.34	2.52 ± 0.15

Notes: More than three independent measurements were carried out. The average values with standard errors are shown.

3.4 | Thermodynamic analysis of the interaction between mAbs and Mut FcγRIIIa using SPR

We next evaluated the interaction between the mAbs and Mut FcγRIIIa, determining the thermodynamic parameters of the interaction between rituximab and Mut FcγRIIIa. SPR analysis was carried out at several temperatures from 10°C to 30°C (Table S3). Based on measured binding affinities, thermodynamic parameters were calculated from van't Hoff plots (Figure 3b,c). Since each R-squared value of van't Hoff plot was greater than 0.99, we did not consider heat capacity changes between free and bound states. The binding entropy of the interaction between Mut FcγRIIIa and Expi293-Rituximab was more favorable than that with ExpiCHO-Rituximab. The higher proportion of galactose residues of N-glycans of Expi293-Rituximab likely

contributed to the more favorable binding entropy. This result is in good agreement with a previous analysis of the impacts of galactose residues.[15] In contrast, the binding enthalpy of Expi293-Rituximab was unfavorable compared with that of ExpiCHO-Rituximab. Similarly, for the interaction with Mut FcγRIIIa the entropy was more favorable and the enthalpy less favorable for Expi293-Trastuzumab compared with ExpiCHO-Trastuzumab (Figure S5).

4 | CONCLUSIONS

We analyzed the glycosylation patterns of monoclonal antibody drugs rituximab and trastuzumab expressed in Expi293 and ExpiCHO cells. There were large differences in chromatograms when Expi293 and

ExpiCHO cell-derived mAbs were analyzed using an FcγRIIIa affinity column. Although the FcγRIIIa expressed on human cells has five N-glycosylation sites, the Mut FcγRIIIa used in affinity separation described here was not glycosylated because it was expressed in *E. coli*. Glycan analysis revealed that mAbs expressed in Expi293 cells have more N-glycans with terminal galactose residues than do ExpiCHO cell-derived mAbs. This difference in the proportion of galactose residues led to different HPLC profiles. The aglycosylated FcγRIIIa ligand may result in the good separation observed. Previously, it was reported that commercially available rituximab is separated into three peaks by the FcγRIIIa affinity column and that the proportion of galactose was highest in the peak that eluted last.[15] We demonstrated here that the FcγRIIIa affinity column profile of Expi293-Rituximab was more similar to that of commercially available rituximab than the rituximab produced in the CHO cell expression system.

We observed no differences in thermal stabilities or in secondary structures in mAbs produced in different cell lines. However, differences in kinetic and thermodynamic parameters of the interaction for between Mut FcγRIIIa and the mAbs that depended on the cell line used for expression were observed. The terminal galactose residues of the N-glycans of the mAbs enhance affinity for FcγRIIIa due to the favorable binding entropy.[15] Both a crystallographic analysis and molecular dynamics simulations revealed that the terminal galactose residues form intramolecular glycan-polypeptide hydrogen bonds,[13,27] and hydrogen-deuterium exchange mass spectrometry analysis indicated that the galactose residues influence the dynamic and conformational ensemble of the IgG-Fc domain.[14,15] Suppression of dynamics of the IgG-Fc domain, particularly the stabilization of C'E loop conformation, enhances affinity for FcγRIIIa.[14,28] Engineering of antibodies to stabilize this glycan-polypeptide interaction can modulate the binding to FcγRIIIa.[29] Because of this mechanism, small differences in the proportion of galactose residues present on mAbs produced in Expi293 and ExpiCHO cells seem to result in different affinities for FcγRIIIa. Interestingly, the binding affinities of Mut FcγRIIIa for rituximab were higher than those of trastuzumab independently of whether the mAbs were expressed in Expi293 or ExpiCHO cells (Table 1). This leads us to hypothesize that the Fab region is an attractive site for IgG engineering to control the binding activity to FcγRIIIa. Actually, there have been several reports showing that the Fab region of IgG influences some binding properties of Fc domain.[14,30-33] Neonatal Fc receptor (FcRn) is known to interact with human IgG1 by different binding affinities depending on varieties of Fab region, though FcRn binds to CH2-CH3 regions of Fc domain.[30,31] The contributions of Fab region to the interaction between IgG and FcγRIIIa were also shown by several researchers.[14,32,33] Especially, high-speed atomic force microscopy and hydrogen-deuterium exchange mass spectrometry demonstrated the direct involvement of Fab region in the interaction between IgG1 and FcγRIIIa, as well as the canonical Fc-mediated interaction.[33] Nevertheless, it should be noted that we did not observe significant differences in the HPLC profiles between rituximab and trastuzumab (Figure 1). This is probably due to the difference in the buffer conditions between SPR and HPLC analyses, suggesting the usefulness of the FcγRIIIa affinity column specialized in the observation of glycosylation patterns. Our data demonstrate that the FcγRIIIa column can be used for rapid and sensitive analysis of glycosylation of mAbs expressed in different cell lines and under different cultivation conditions without need for complicated and time-consuming glycan analysis. An FcγRIIIa column is commercially available from TOSOH (Tokyo, Japan) as TSKgel FcR-IIIA-NPR. Traditionally, LC–MS/MS, and fluorescence UPLC analysis have been used to evaluate the N-glycosylation of antibody drugs of each production lot. These methods are, however, time-consuming and expensive and are not suitable for high-throughput, real-time monitoring of the production process. Whereas the reproducibility of the FcγRIIIa column was succeeded when using the same lot of samples and running buffer, shapes of observed peaks are likely to be subject to subtle differences of buffer condition (Figure 1; Figure S1). However, the significant changes in percentages of peak areas were not observed when comparing the measurements using a different lot of samples and running buffer, in spite of the different shapes of peaks (Table S4). Our work indicates that the FcγRIIIa affinity column is easy in handling and sensitive monitoring of the glycosylation of mAbs during the optimization of expression condition.

NOTATION

CD	circular dichroism
CHO	Chinese hamster ovary
DSC	differential scanning calorimetry
DSF	differential scanning fluorimetry
FcγR	Fcγ receptor
HEK	human embryonic kidney
HPLC	high-performance liquid chromatography
IgG	immunoglobulin G
mAb	monoclonal antibody
RU	resonance units
SPR	surface plasmon resonance

ORCID

Satoru Nagatoishi https://orcid.org/0000-0002-0794-3963
Masato Kiyoshi https://orcid.org/0000-0002-5969-8138
Kouhei Tsumoto https://orcid.org/0000-0001-7643-5164

REFERENCES

1. Walsh G. Biopharmaceutical benchmarks 2018. *Nat Biotechnol*. 2018; 36:1136-1145.
2. Kaplon H, Muralidharan M, Schneider Z, Reichert JM. Antibodies to watch in 2020. *mAbs*. 2020;12:1703531.
3. Ecker DM, Jones SD, Levine HL. The therapeutic monoclonal antibody market. *mAbs*. 2015;7:9-14.

4. U.S. Food and Drug Administration. *Purple Book: Lists of Licensed Biological Products with Reference Product Exclusivity and Biosimilarity or Interchangeability Evaluations*. USA: FDS; https://www.fda.gov/drugs/therapeutic-biologics-applications-bla/purple-book-lists-licensed-biological-products-reference-product-exclusivity-and-biosimilarity-or. Accessed April 5, 2020.

5. Lowe D, Dudgeon K, Rouet R, Schofield P, Jermutus L, Christ D. Aggregation, stability, and formulation of human antibody therapeutics. *Adv Protein Chem Struct Biol*. 2011;84:41-61.

6. Fukada H, Tsumoto K, Arakawa T, Ejima D. Long-term stability and reversible thermal unfolding of antibody structure at low pH: case study. *J Pharm Sci*. 2018;107:2965-2967.

7. Vlasak J, Ionescu R. Fragmentation of monoclonal antibodies. *mAbs*. 2011;3:253-263.

8. Shibata H, Nishimura K, Miyama C, et al. Comparison of different immunoassay methods to detect human anti-drug antibody using the WHO erythropoietin antibody reference panel for analytes. *J Immunol Methods*. 2018;452:73-77.

9. Jennewein MF, Alter G. The immunoregulatory roles of antibody glycosylation. *Trends Immunol*. 2017;38:358-372.

10. Kiyoshi M, Tsumoto K, Ishii-Watabe A, Caaveiro JMM. Glycosylation of IgG-Fc: a molecular perspective. *Int Immunol*. 2017;29:311-317.

11. Jefferis R. Glycosylation as a strategy to improve antibody-based therapeutics. *Nat Rev Drug Discov*. 2009;8:226-234.

12. Okazaki A, Shoji-Hosaka E, Nakamura K, et al. Fucose depletion from human IgG1 oligosaccharide enhances binding enthalpy and association rate between IgG1 and FcγRIIIa. *J Mol Biol*. 2004;336:1239-1249.

13. Raju TS. Terminal sugars of Fc glycans influence antibody effector functions of IgGs. *Curr Opin Immunol*. 2008;20:471-478.

14. Houde D, Peng Y, Berkowitz SA, Engen JR. Post-translational modifications differentially affect IgG1 conformation and receptor binding. *Mol Cell Proteomics*. 2010;9:1716-1728.

15. Kiyoshi M, Caaveiro JMM, Tada M, et al. Assessing the heterogeneity of the Fc-glycan of a therapeutic antibody using an engineered FcγReceptor IIIa-immobilized column. *Sci Rep*. 2018;8:3955.

16. Yamaguchi Y, Nishimura M, Nagano M, et al. Glycoform-dependent conformational alteration of the Fc region of human immunoglobulin G1 as revealed by NMR spectroscopy. *Biochim Biophys Acta*. 2006;1760:693-700.

17. Thomann M, Schlothauer T, Dashivets T, et al. *In vitro* glycoengineering of IgG1 and its effect on Fc receptor binding and ADCC activity. *PLoS One*. 2015;10:e0134949.

18. Solá RJ, Griebenow K. Effects of glycosylation on the stability of protein pharmaceuticals. *J Pharm Sci*. 2009;98:1223-1245.

19. Kayser V, Chennamsetty N, Voynov V, Forrer K, Helk B, Trout BL. Glycosylation influences on the aggregation propensity of therapeutic monoclonal antibodies. *Biotechnol J*. 2011;6:38-44.

20. Clynes RA, Towers TL, Presta LG, Ravetch JV. Inhibitory Fc receptors modulate in vivo cytotoxicity against tumor targets. *Nat Med*. 2000;6:443-446.

21. Egashira Y, Nagatoishi S, Kiyoshi M, Ishii-Watabe A, Tsumoto K. Characterization of glycoengineered anti-HER2 monoclonal antibodies produced by using a silkworm–baculovirus expression system. *J Biochem*. 2018;163:481-488.

22. Goh JB, Ng SK. Impact of host cell line choice on glycan profile. *Crit Rev Biotechnol*. 2018;38:851-867.

23. Jain NK, Barkowski-Clark S, Altman R, et al. A high density CHO-S transient transfection system: comparison of ExpiCHO and Expi293. *Protein Expr Purif*. 2017;134:38-46.

24. Sou SN, Sellick C, Lee K, et al. How does mild hypothermia affect monoclonal antibody glycosylation? *Biotechnol Bioeng*. 2015;112:1165-1176.

25. Fan Y, Jimenez Del Val I, Müller C, et al. Amino acid and glucose metabolism in fed-batch CHO cell culture affects antibody production and glycosylation. *Biotechnol Bioeng*. 2015;112:521-535.

26. Johnson CM. Differential scanning calorimetry as a tool for protein folding and stability. *Arch Biochem Biophys*. 2013;531:100-109.

27. Fortunato ME, Colina CM. Effects of galactosylation in immunoglobulin G from all-atom molecular dynamics simulations. *J Phys Chem B*. 2014;118:9844-9851.

28. Subedi GP, Barb AW. The structural role of antibody N-glycosylation in receptor interactions. *Structure*. 2015;23:1573-1583.

29. Chen W, Kong L, Connelly S, et al. Stabilizing the CH2 domain of an antibody by engineering in an enhanced aromatic sequon. *ACS Chem Biol*. 2016;11:1852-1861.

30. Wang W, Lu P, Fang Y, et al. Monoclonal antibodies with identical Fc sequences can bind to FcRn differentially with pharmacokinetic consequences. *Drug Metab Dispos*. 2011;39:1469-1477.

31. Jensen PF, Schoch A, Larraillet V, et al. A two-pronged binding mechanism of IgG to the neonatal Fc receptor controls complex stability and IgG serum half-life. *Mol Cell Proteomics*. 2017;16:451-456.

32. Shi L, Liu T, Gross ML, Huang Y. Recognition of human IgG1 by Fcγ receptors: structural insights from hydrogen-deuterium exchange and fast photochemical oxidation of proteins coupled with mass spectrometry. *Biochemistry*. 2019;58:1074-1080.

33. Yogo R, Yamaguchi Y, Watanabe H, et al. The Fab portion of immunoglobulin G contributes to its binding to Fcγ receptor III. *Sci Rep*. 2019;9:11957.

SUPPORTING INFORMATION

Additional supporting information may be found online in the Supporting Information section at the end of this article.